

A framework for national-scale predictions of forage dry mass in Senegal: UAVs as an intermediate step between field measurements and Sentinel-2 images

Maïalichah Nungi-Pambu, Adama Lo, Cofélas Fassinou, Torbern Tageson, Rasmus Fensholt, Abdoul Aziz Diouf, Jean Baptiste Menassol, Mohammed Habibou Assouma, Ibra Toure & Simon Taugourdeau

To cite this article: Maïalichah Nungi-Pambu, Adama Lo, Cofélas Fassinou, Torbern Tageson, Rasmus Fensholt, Abdoul Aziz Diouf, Jean Baptiste Menassol, Mohammed Habibou Assouma, Ibra Toure & Simon Taugourdeau (15 Dec 2023): A framework for national-scale predictions of forage dry mass in Senegal: UAVs as an intermediate step between field measurements and Sentinel-2 images, International Journal of Remote Sensing, DOI: [10.1080/01431161.2023.2290992](https://doi.org/10.1080/01431161.2023.2290992)

To link to this article: <https://doi.org/10.1080/01431161.2023.2290992>



Published online: 15 Dec 2023.



Submit your article to this journal [↗](#)



View related articles [↗](#)



View Crossmark data [↗](#)



A framework for national-scale predictions of forage dry mass in Senegal: UAVs as an intermediate step between field measurements and Sentinel-2 images

Maïalichah Nungi-Pambu^{a,b}, Adama Lo^c, Cofélas Fassinou^d, Torbern Tageson^{e,f}, Rasmus Fensholt^f, Abdoul Aziz Diouf^c, Jean Baptiste Menassol^b, Mohammed Habibou Assouma^{a,g}, Ibra Toure^{a,g} and Simon Taugourdeau^{a,g,h}

^aCIRAD UMR SELMET- PPZS, Dakar, Senegal; ^bSELMET, L'Institut Agro Montpellier, CIRAD, INRAE, Univ Montpellier, Montpellier, France; ^cCentre de Suivi Ecologique, PPZS, Dakar, Senegal; ^dISRA, CRZ (Centre de Recherches Zootechniques), Dahra-PPZS, Dahra Djoloff, Senegal; ^eDepartment of Physical Geography and Ecosystem Science, Lund University, Lund, Sweden; ^fDepartment of Geosciences and Natural Resource Management, University of Copenhagen, Copenhagen, Denmark; ^gUMR SELMET, CIRAD, INRA Institut Agro, Univ Montpellier, Montpellier, France; ^hUMR AMAP Univ Montpellier, CIRAD, CNRS, INRAE, IRD, Montpellier, France

ABSTRACT

Monitoring available feed for livestock is a key factor for developing pastoralism in the Sahel, and satellite images has proven useful in monitoring dry mass on large spatial scales. This approach requires field measurements of dry mass (herbaceous and woody plants) to calibrate such models based on Earth observation data. However, the need for representative field measurements can be a challenge when considering the low spatial resolution of available satellite data. Unmanned Aerial Vehicles (UAV) can produce very high-resolution images, so we tested UAVs as an intermediate step between field measurements and satellite images, to bridge the difference in spatial scale. We used 43 orthomosaics from a red-green-blue (RGB) UAV sensor in combination with field measurements of herbaceous and woody dry biomass at sites located primarily in the northern/central and southernmost parts of Senegal. We developed a dry mass model trained with field observed measurements to be applied on the UAV orthomosaics. The dry mass information obtained from these UAV maps was subsequently related to vegetation indices derived from Sentinel-2 data to produce a national-scale 10 m spatial resolution baseline map of herbaceous and woody dry mass for Senegal in 2020. We obtained a high correlation between dry mass derived from UAV and Sentinel-2 indices ($R^2 = 0.91$), suggesting a robust basis for national-scale mapping. Lastly, our map was compared with a state-of-the-art annual reference map based on satellite remote sensing. This comparison showed a difference of 21 million tons of dry mass at national level. We concluded that bridging the spatial gap between field and satellite observations using spatially representative UAV data collection is a cost-effective approach for accurate mapping of dry mass at national level using freely available Sentinel-2 satellite data.

ARTICLE HISTORY

Received 9 July 2023

Accepted 13 November 2023

1. Introduction

The Sahel is a transition zone between the Sahara Desert in the North and a humid climate in the Sudanian Savanna in the South covering six different countries (Mauritania, Senegal, Burkina Faso, Mali, Niger and Chad). The rainfall gradient in all the countries typically varies from the driest regions in the North to the wetter regions in the South. In Senegal, the focus of this study, rainfall ranges from an average of 200 mm/ha in the North to 1,200 mm/ha in the South (Tappan et al. 2004). A distinct feature of the climate in Sahelian countries is a concentration of rainfall in the rainy season, typically lasting from around June to October, with the rest of the year being the dry season. However, the exact timing of the rainy season, and the amount of rainfall, can vary considerably between years (Janowiak 1988; L'Hote et al. 2002).

The ecosystem type varies from Sahelian steppes in the North to dry tropical forests in the South, but most of the area is covered by savanna. The savanna ecosystem is composed of a herbaceous layer (annual or perennial species) and a sparse woody community (Le Houerou 1980). This vegetation resource produces many ecosystem services supporting the livelihoods of the local population (Hanan et al. 2021; Wessels et al. 2013), particularly through livestock farming. Livestock practices have adapted to the spatio-temporal variations in environmental feed availabilities (in terms of both quantity and quality), making extensive pastoral systems the dominating livelihood system. In this region, livestock management is governed by the rainfall in the wet season, during which the animals take advantage of the high nutritional value of the rangelands' herbaceous strata (Ayantunde et al. 1999) to store body fat reserves. These reserves are gradually brought into play during the long dry season to compensate for the poor digestibility of forage and attenuate losses in nutritional status (Ezanno, Ickowicz, and Bocquier 2003). At the end of the dry season, woody foliar dry mass constitutes the main feed resource (Assouma et al. 2018). In order to cope with resource scarcity, herders have developed various strategies, such as daily feeding planning and seasonal transhumance within the country (Gaston and Lamarque 1994). Vegetation growth in Sahelian rangelands is driven by the highly seasonal rainfall provided by the convective storms of the West African monsoon. Assessing dry mass (i.e. natural feed) across large scales (regions, countries or even larger scales) is a key goal for livestock management, especially for national and international policy (Touré and Ickowicz 2014). This information can be used to identify pastoral crises (forage deficits) and manage livestock mobility.

Satellite remote sensing is commonly used to evaluate and spatialize dry mass across the different Sahelian countries. Some studies have used vegetation indices as a proxy to evaluate dry mass dynamics and compare them over different years (Fensholt and Rasmussen 2011; Fensholt et al. 2009). Other remote sensing-based approaches rely on field measurements and calibrating field measurements of dry mass with vegetation indices (Diouf et al. 2016; Garba et al. 2017). However, in order to be upscaled, such field measurements need to be representative given the spatial resolution of satellite imagery (Diouf et al. 2015). The first studies in Senegal were launched at the end of the 1980's with satellite imagery data of moderate spatial resolution (pixels of 1 km spatial resolution) (Diouf et al. 2016). Due to the high heterogeneity of the vegetation in savanna ecosystems, the protocols developed to ensure this representativeness were therefore labour- and time-consuming. Different

protocols have been proposed and applied in a Sahelian context, but they have generally been based on measuring at least twenty 1 m² plots of grass and several plots with complete inventories of the woody community for one single site (Hiernaux et al. 2016). Such intensive field work makes it difficult for the different countries to quantify available dry mass (Hiernaux et al. 2016).

One option for potentially overcoming the challenge of point-to-pixel comparison in highly heterogeneous landscapes is to use very high spatial resolution images (VHR) taken from unmanned aerial vehicles (UAV). Using UAVs is a low-cost and efficient way of producing VHR resolution estimates of biomass covering several hectares (Grenzdörffer, Engel, and Teichert 2008; Kaneko and Nohara 2014). Furthermore, UAV data can be combined with field measurements in such a way that the time differences between imagery and field measurements are minimized. Lastly, UAV use is not restricted to cloud-free conditions only.

Many studies have shown that UAV outputs can be linked to dry herbaceous and woody mass (Bendig et al. 2015; Bossoukpe et al. 2021, 2021; Lussem et al. 2018; Mayr et al. 2018; Taugourdeau et al. 2022; Wijesingha et al. 2020). First, a model has to be developed linking field measurements to VHR images (Taugourdeau et al. 2014) from which VHR maps of the dry mass can be produced. The map can subsequently be used as input to build a relationship with satellite imagery with a medium-high spatial resolution (>10 m) covering larger areas. Another advantage of using VHR is the possibility of separating tree cover and herbaceous cover in the savanna ecosystem (Brandt et al. 2020), when building empirical models.

In this context, the aim of this study was to test the applicability of UAVs as an intermediate step to bridge the difference in spatial scale between field and satellite observations, ultimately for better mapping of forage dry mass on large spatial scales in the Sahel.

2. Material and methods

We used datasets from various sources combining UAV outputs with field measurements taken from the northern/central to southern parts of Senegal (Figure 1).

The workflow (Figure 2) involved: 1) Segmentation to separate the woody and herbaceous parts from the different UAV orthomosaics. 2) Application of two models (one linear regression and one random forest model) to produce total dry mass for the herbaceous and woody vegetation layers. 3) Calculation of vegetation indices based on Sentinel-2 data corresponding to the locations of the UAV orthomosaics. 4) Finally, development of a random forest model to predict the dry mass of the two layers combined at national level using the total biomass derived from the UAV model and the Sentinel-2 vegetation indices as the dependent variables.

2.1. UAV data collection and processing

We used a UAV dataset collected in 2020 in the northern/central and southern parts of Senegal covering 43 different sites (Figure 1). For each site, a flight was made with a Parrot ANAFI UAV (<https://www.parrot.com>). The flight was controlled with PIX4Dcapture software (www.pix4d.com/). The altitude was set to 80 m above the

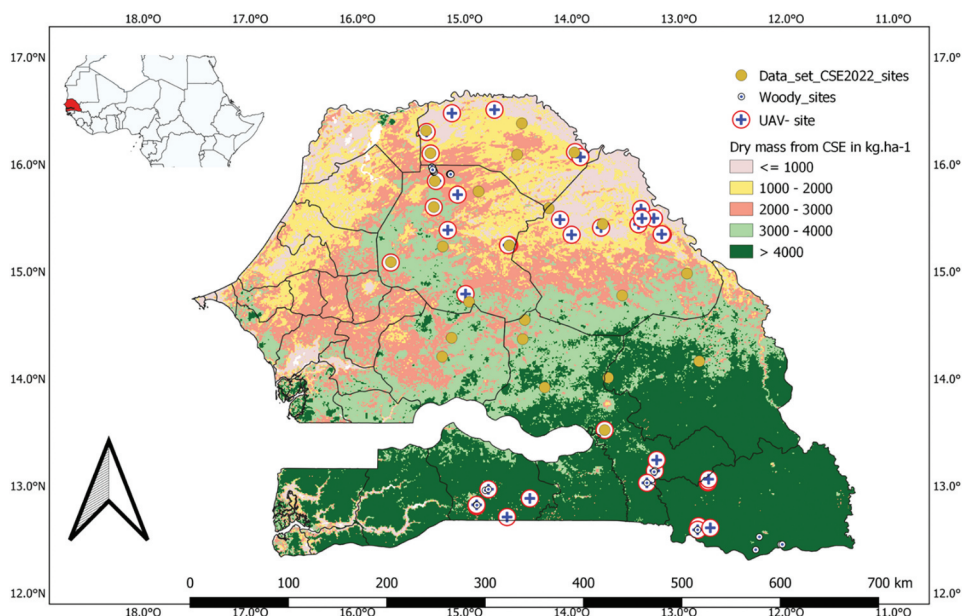


Figure 1. Locations of the different data used. The map represents the dry mass in kg per ha (herbaceous and woody) based on the Centre de Suivi Ecologique (CSE) in 2020 (following their methodology; source CSE). The UAV sites represent the sites used for herbaceous dry mass calibration and the scaling-up with Sentinel-2 images. The CSE sites were used for the creation of the CSE map and for the woody calibration. The woody sites were used for the woody dry mass calibration.

ground, and we used a double grid flight plan with 80% of overlap between flight lines. The data were subsequently analysed using PIX4D mapper software to produce a crown height model (CHM) and an orthomosaic with RGB colours. Different vegetation indices were calculated based on the spectral reflectance values of the RGB bands (Table 1).

UAV maps can have some geotag inaccuracies due to the quality of the GNSS signal (ANAFI do not have an on-board Real Time Kinematic or RTK algorithm for GNSS data correction). We corrected the georeferencing of the different UAV images using images from Google Satellite Hybrid (@Google) and used the location of trees, and in some cases human traces, as tie-points (conducted in QGIS 3.16). For each image to be georeferenced, we produced multiple tie-points as close as possible to all four image corners, to avoid excessive deformation. We kept the default transformation parameters and the local system coordinates.

The second step of image preprocessing was the segmentation between woody cover and herbaceous or ground soil cover. We used the crown height model (CHM; difference between digital surface model or DSM and digital terrain model, or DTM). The herbaceous layer in the Sahel region generally has a maximum height of 0.50–1 m (Diatta et al. 2023), and consequently in the northern region (all sites starting with N# in Figure 1), we defined all pixels in the CHM >1 m to belong to the woody layer. For the southern region (all sites starting with S# in Figure 1), we used a 1.5 m threshold due to the existence of taller herbaceous species in this region based on our field measurements. As bushes were lower

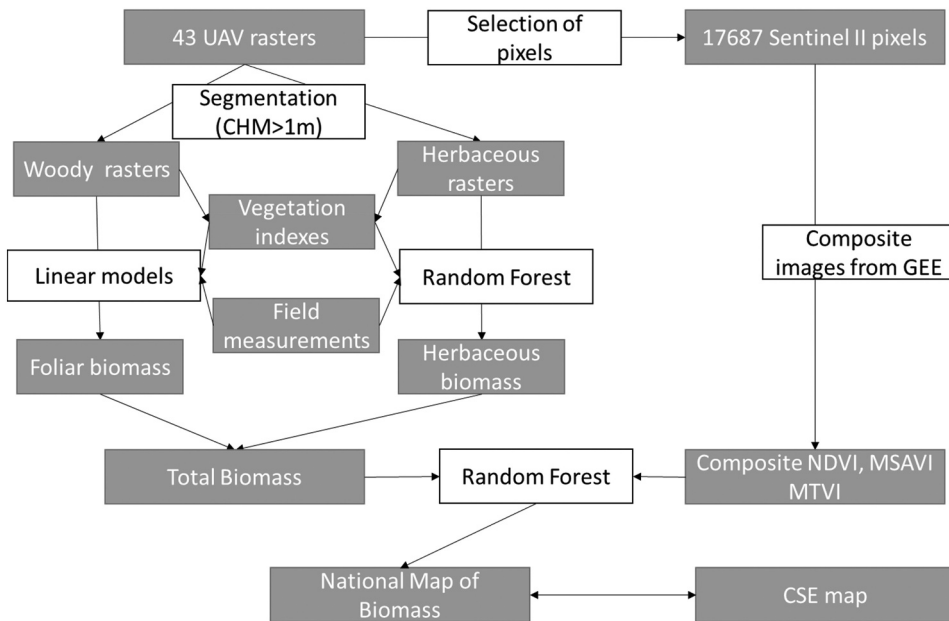


Figure 2. Workflow of the data analysis. The gray boxes correspond to the data and the white boxes to the different analyses carried out.

Table 1. Different vegetation indices (G Green, R red, B blue) from the UAV imagery applied in the study.

Acronym	Definition	Formulas	References
GR	Normalized Difference Green Red Index	$(R-G)/(R+G)$	Inspired from NDVI (Rouse et al. 1973)
GB	Normalized Difference Blue Green Index	$(B-G)/(B+G)$	Inspired from NDVI (Rouse et al. 1973)
RB	Normalized Difference Blue Red Index	$(B-R)/(B+R)$	Inspired from NDVI (Rouse et al. 1973)
Vari	Visible Atmospheric Resistant Index	$(G-R)/(G+R-B)$	
Exg	Excess of green	$G-0.39*R-0.61*B$	(Bassine, Errami, and Khaldoun 2019)
Gli	Green Leaf Index	$(2*G-R-B)/(2*G+R+B)$	(Bassine, Errami, and Khaldoun 2019)

than these two threshold values, they were assigned to the herbaceous layer, which inevitably induced some uncertainty in the final dry mass model.

All Sentinel-2 pixels overlapping the UAV orthomosaics were used for further analysis. However, for some UAV images, the edges were badly processed and the corresponding Sentinel-2 pixels were excluded.

2.2. Dry mass data used for model calibration

2.2.1. Herbaceous dry mass

For all study sites (Figure 1), herbaceous vegetation was collected at the end of the 2020 rainy season. Measurements were taken in one to three 1 m^2 plots for each of the sites where UAV flights were conducted. The herbaceous vegetation collected was subsequently dried for 48 hours at 55°C to obtain the dry mass. In total, this procedure was carried out for 86 plots across Senegal. The calibration between herbaceous dry mass and the UAV outputs from this dataset was published in Taugourdeau et al. (2022) and we

used a random forest model (Breiman 2001) to create a model between herbaceous biomass and UAV outputs. Random forest is a set of many regression trees. For each run, only one part of the data and some of the variable are used. The rest of the data is used for cross validation. The random forest can be deal with the collinearity.

2.3. Woody foliar dry mass

For the woody foliar dry mass, we used other datasets collected separately by using a plot level approach (square or circular plot). We included 84 inventory plots obtained from three different datasets:

- The CSE (*Centre de Suivi Ecologique* in Dakar) monitored the woody foliar dry mass at 24 sites across the northern and eastern parts of Senegal (Figure 1). For each site, woody inventories were conducted in April 2022 in two circular plots with a 20.0 m and 24.5 m radius, respectively, depending on tree density. During this campaign, UAV flights were conducted with a DJI mavic pro (DJI) at each of these sites. The flights were undertaken at a height of 80 m, covered an area of 1 ha, and had a double grid with 80% of overlap.
- In August 2021, we carried out tree inventories in 24 plots with an area of $50 \times 50 \text{ m}^2$ in the northwestern part of Senegal (Figure 1). For each of these six sites, two 10-ha squares were selected at the beginning and end of a 1000 m-long transect. In each large square, two plots were selected based on visual interpretation from Bing Images (@Bing): one with low and high tree density, respectively. For each of these 24 plots, all woody individuals with a circumference over 10 cm at a height of 30 cm were counted and the trunk circumference 30 cm from the ground was measured for each of the stems. In these 24 plots, UAV flights were carried out in November 2021, with an ANAFI UAV (80 m altitude, 90% of overlap, double grid on $70 \text{ m} \times 75 \text{ m}$).
- In November 2021, we carried out tree inventories in 12 plots in the southern part of Senegal. The sites were selected to cover the ecosystem diversity of the region (forest, savanna, fallow, steppes). Plot sizes were either $50 \times 50 \text{ m}$ or $30 \times 30 \text{ m}$, depending on the density of the vegetation ($50 \times 50 \text{ m}$ for open ecosystems and $30 \times 30 \text{ m}$ for forest). Within each plot, the circumference was measured for all woody individuals with a circumference over 10 cm at a height of 1.3 m. Flights were made with an ANAFI UAV (80 m altitude, 90% of overlap, double grid on $100 \times 100 \text{ m}$) at the same time as the inventory was undertaken.

From all the inventory data, we used allometric equations to calculate the foliar dry mass for each tree. The list of the allometric equations used are presented in supplementary data files. We summed up the dry mass for each plot to obtain the dry mass at plot level, divided by the area of the plot, to obtain a dry mass value per ha. The UAV orthomosaics were segmented with the CHM using the same threshold as for the image of 2020 (0 m for northern sites and 1.5 m for southern sites; subsection A above). We estimated the average reflectance for each band in the UAV images for the canopy part of each plot and calculated the same indices as used for herbaceous vegetation (Table 1). Linear models were parameterized using the UAV outputs (Table 1) and CH and foliar dry mass at plot level using a stepwise regression in both directions. The output of the stepwise

regression was a linear model between dry mass per ha and the different variables from the UAV. Due to the lower number of points and the unbalanced distribution, we were not able to use a random forest method. We did not make cross validation for foliar woody dry mass.

2.4. Satellite image and model development

All Sentinel-2 pixels overlapping the UAV orthomosaics were used for further analysis. However, for some UAV images, the edges were badly processed and the corresponding Sentinel-2 pixels were excluded.

Two models (random forest for herbaceous dry mass and linear model for woody foliar dry mass) were applied respectively on each part of a given orthomosaic based on the segmentation presented in part A (threshold on the CHM).

For the herbaceous layer, we divided the orthomosaic into a grid with a pixel size of 1 m². The average values of the UAV-based vegetation indices were calculated for all 1 m² grid cells. For squares that also included a woody part, the average value was calculated only on the part containing herbaceous information and subsequently applied to the entire square. We assumed here that the herbaceous dry mass at the edge (vertical projection) of the crown was similar to the dry mass under the tree (Fassinou et al. 2022). However, the areas under the tree crowns were set as no data. Finally, we aggregated the estimated dry herbaceous mass to the spatial scale of Sentinel-2 by averaging the dry mass of the different 1 m² pixels for each pixel.

For the woody part of the orthomosaic, we used the 10 m × 10 m Sentinel pixel. For each pixel, we extracted the average reflectance (with 0 for the non-woody part) and calculated the different indices. A linear model was applied to the 10 m × 10 m pixel to predict the foliar dry mass per ha for each pixel.

We add to different sampling sizes for the herbaceous and the woody dry mass to fit with measurement sampling size. Furthermore, the spatial heterogeneity of herbaceous and woody plant is not the same in savannah ecosystem.

We used L2A Sentinel-2 images from the Google Earth Engine (GEE) collection. The Level-2A product is derived from the Level-1C product and provides atmospherically corrected surface reflectance images. We used the QA60 process to overcome influence from cloud cover. We produced a composite of Sentinel-2 imagery from June to November for 2020 using GEE. For each pixel, we calculated three vegetation indices: NDVI, MSAVI 2 and MTVI 2. We used with vegetation indices based on the work of Lo et al. (2022).

We used a random forest model to explain the dry mass obtained from UAV imagery with the vegetation indices derived from Sentinel-2 data (Breiman 2001).

2.5. Comparison with the CSE national map

The *Centre de Suivi Ecologique* (CSE) has been routinely monitoring the dry mass of Senegal since the 1980's. Twenty-four sites are monitored each year in the northern and central parts of Senegal (Figure 1). Herbaceous dry mass is measured by stratified sampling along a 1 km transect. Along the 1 km, the level of dry mass is evaluated visually (bare soil, low, medium, high) for each metre. For each of the different levels, the herbaceous mass is collected in a 1-m square from a random sample. The mass is

subsequently dried to obtain the dry mass. Here, along the transects, four circular plots were positioned at 200 m, 400 m, 600 m and 800 m. The area of the plots depended on the density of the woody individuals (either 1/16 or 1/4 ha). Inventories of all woody individuals were conducted every few years (2–4 years). Allometric equations based on trunk circumferences were used to quantify foliar dry mass (see supplementary data files). The average total dry mass for each site was obtained by summing up the average herbaceous and foliar dry masses (Diouf et al. 2015, 2016). The CES used NDVI 300 m V2 (Sentinel-3/OLCI) of the Copernicus Global Land Service (CGLS) platform (<https://land.copernicus.eu/>), resampled to 1 km² spatial resolution and extracted from the area around the 1 km transect (3 km by 3 km). An ordinary linear model was parameterized with dry mass from the inventory plots and these NDVI estimations. Lastly, the linear model was applied to estimate total dry mass on a national scale with a spatial resolution of 1 km. Here we only used the map produced in 2020.

3. Results

3.1. Models predicting dry herbaceous and woody foliar masses

3.1.1. Modeling herbaceous dry mass

The random forest model applied on the herbaceous dry mass field measurements and UAV vegetation index outputs explained 58.64% of the variability in field dry mass (Figure 3). This model was similar to the model published in the paper by Taugourdeau et al. (2022).

3.1.2. Woody dry mass modeling

For the plot scale model (Figure 4), only one variable was selected by the stepwise regression, namely the exg index (Table 1). The best model was:

$$\text{dry mass(g/m}^2\text{)} = 25.60 \cdot \text{exg} + 22.74; R^2 = 0.73 \text{ (p-value } < 0.05\text{)}$$

For the subsequent analyses we used the plot-based model for the woody mass predictions.

3.2. UAV herbaceous and woody foliar dry mass estimation

The herbaceous dry mass obtained from the random forest-based model (Figure 5) for the 43 UAV orthomosaics generally showed a pronounced difference between the mass of the northern and the southern sites (Figure 5). The dry mass values shown represent the average 1 m² grids from the UAV layer corresponding to the 10 m spatial resolution of the Sentinel-2 pixel encompassing each of the sites. The northern sites (drier) generally revealed a lower herbaceous dry mass (136.81 g.m²) than the southern sites (wetter) (195.26 g.m²). However, some sites in southern Senegal also had lower herbaceous dry mass (the lowest site had an average of 107 g.m²). The variability within each site was large in relation to the scalability of ground observations, and the average coefficient of variation (CV) was 23.3% for the 45 sites (the lowest CV reached 6% and the highest reached 52%). This high degree of heterogeneity is one factor that could add noise when performing a direct calibration of satellite observations from field measurements.

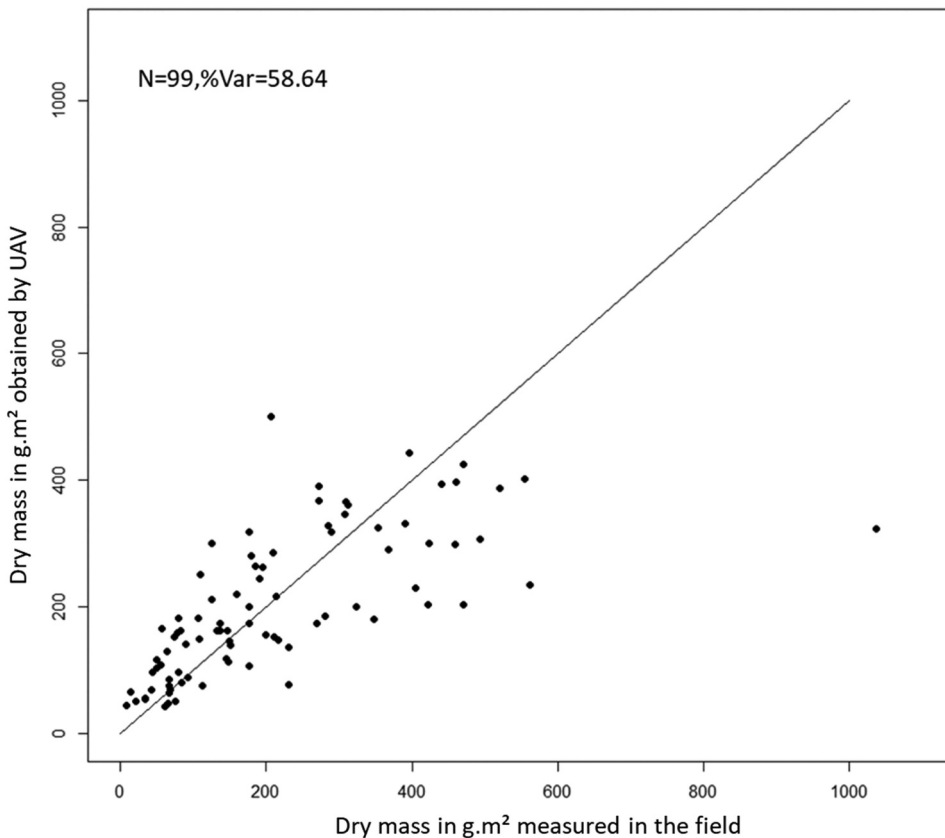


Figure 3. Relationship between herbaceous dry mass measured in the field and the UAV-based prediction of herbaceous dry mass. Each point represents the measurement of the herbaceous dry mass from a 1 m² plot. Var represents the percentage of variability explained by the random forest algorithm as a %.

The woody foliar dry mass was found to be highly variable between and within sites (the latter only in some cases) (Figure 6). Some sites had no woody cover, so woody foliar dry mass equalled zero, whereas some sites had a high woody cover, with the highest observed woody foliar dry mass being 147.77 g.m². The foliar dry mass was generally lower in the northern part of Senegal (average of the mean site value of 33.65 g.m⁻² with an average CV of 95%) than in the southern part (average of the mean site value of 95.57 g.m⁻² with an average CV of 49%).

The distribution of the total estimated dry mass (herbaceous dry mass and foliar dry mass) obtained by the addition of both estimates for a pixel (10 m × 10 m) showed high variability between sites (Figure 7). The sites with the lowest dry mass had an average value of 117.g.m⁻² and the highest value was found to be 527.34 g.m⁻². The average coefficient of variation was 41% (the lowest for a site was 13% and the highest 72%). We used these data from the different sites to calibrate to Sentinel-3 images.

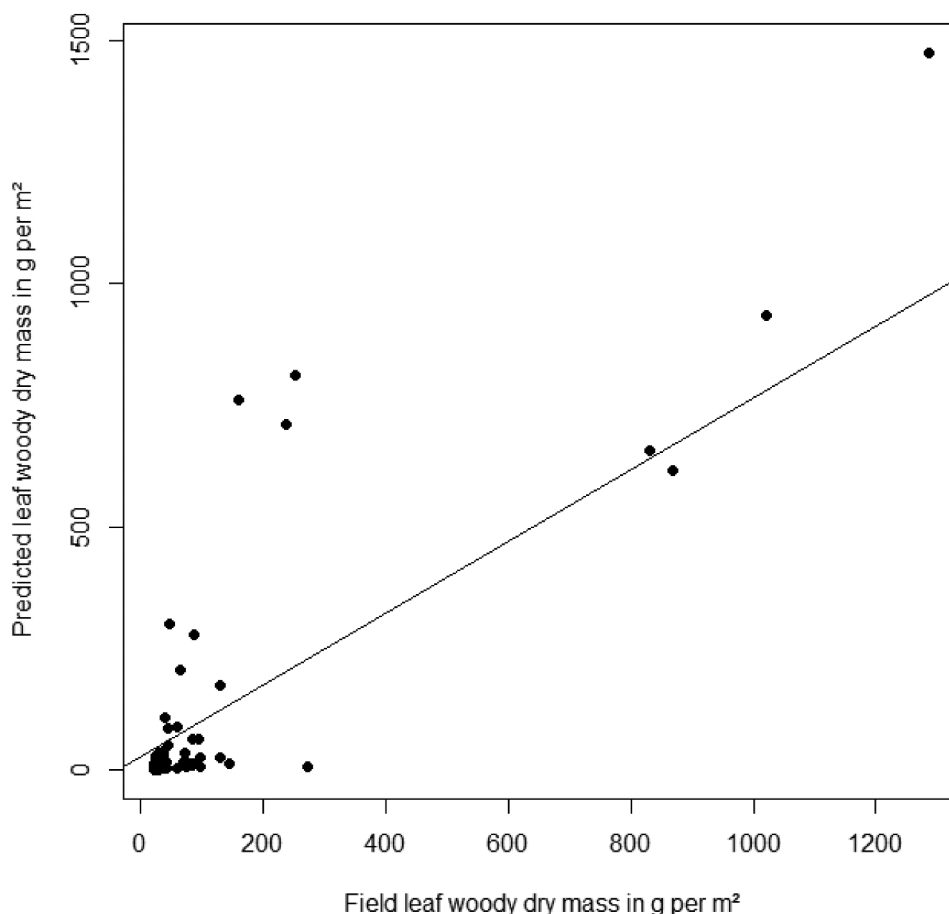


Figure 4. Predicted woody dry mass from the plot-based model versus field-measured dry mass.

3.3. National-scale dry mass map based on Sentinel-2

The random forest model predicting dry mass based on the NDVI, MSAVI and MTVI from Sentinel-2 explained 91% of the variance of the dry mass estimated by UAV (used as training for the model) (Figure 8)

The random forest model was subsequently applied on the composite image of NDVI, MSAVI and MTVI from Sentinel-2 for the whole of Senegal to produce a map of dry mass on a national scale (Figure 9). We call this map UAV lao. The overall dry mass nationally was estimated at 463,284,948 tons, with an average dry mass of 2,243 kg per ha. The lowest average dry mass was found in the Fatick Region with 1,810 kg.ha⁻¹ followed by the Saint Louis region with 1,818 kg.ha⁻¹. The highest was found for the Kolda Region with 2,986 kg.ha⁻¹ followed by the region of Ziguinchor with 2,723 kg.ha⁻¹.

The CSE dry mass map produced for 2020 (Figure 1) was used as a reference to compare with our map (UAV map). The sum of the dry mass was equivalent to 66,885,956 t with an average of 2,243.63 kg. ha⁻¹. The lowest dry mass was found in the Dakar Region with a value of 789.31 kg.ha⁻¹ (corresponding to 2,003.43 kg.ha⁻¹ in the UAV

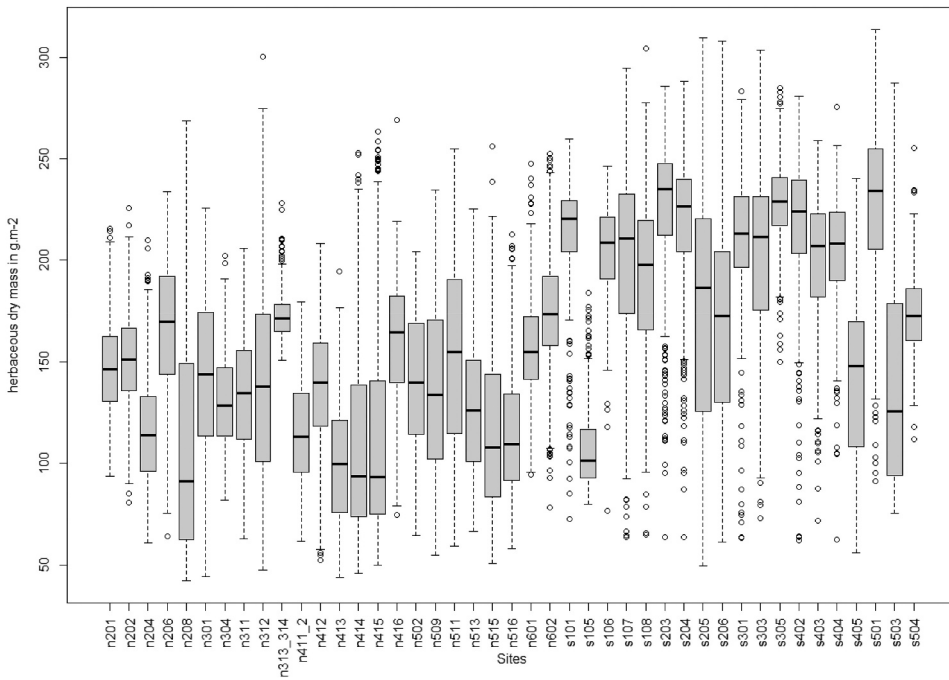


Figure 5. Herbaceous dry mass for the 43 different sites. The box plots represent the distribution of the 10 m * 10 m herbaceous dry mass within each different site. The bars represent the median values and the circles are outliers.

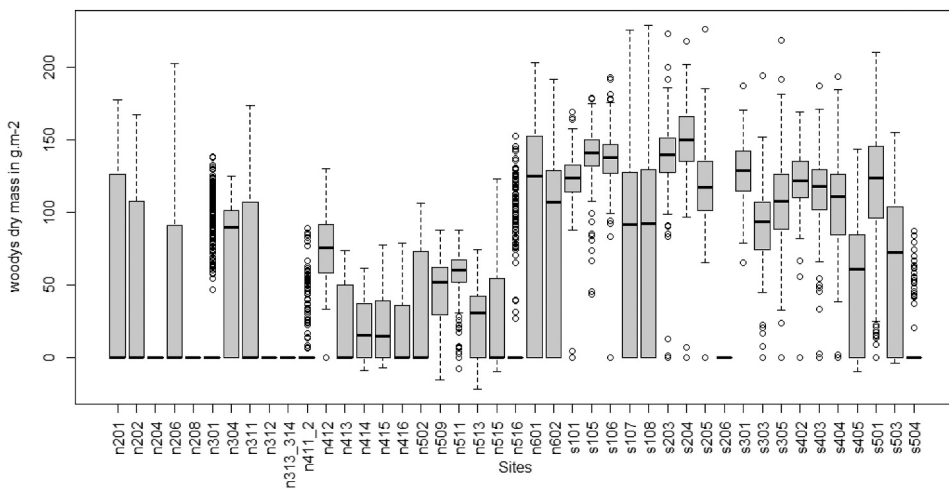


Figure 6. Woody foliar dry mass for the different sites. The box plots represent the distribution of the 10 m * 10 m woody foliar dry mass within each of the different sites. The bars represent the median values and the circles are outliers.

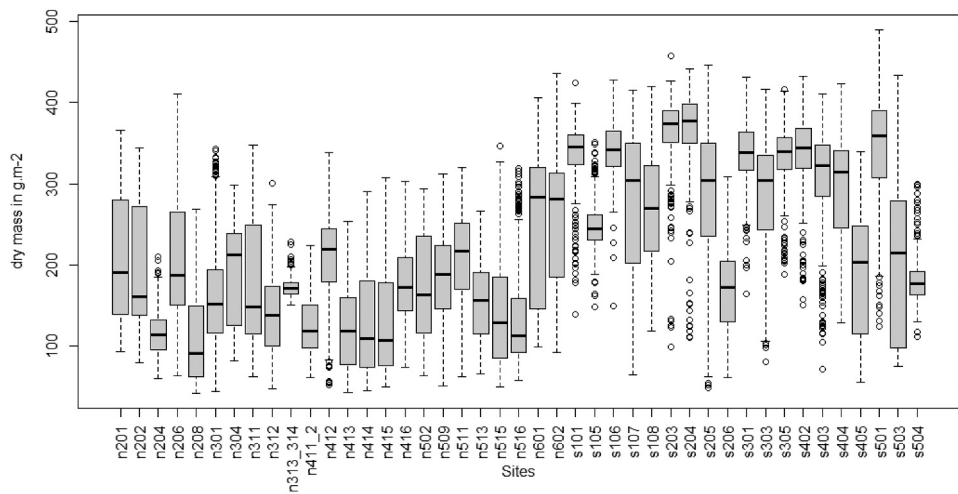


Figure 7. Total dry mass (herbaceous and woody foliar) for the different sites. The box plots represent the distribution of the 10 m * 10 m woody foliar dry mass within each of the different sites. The bars represent the median values and the circles are outliers.

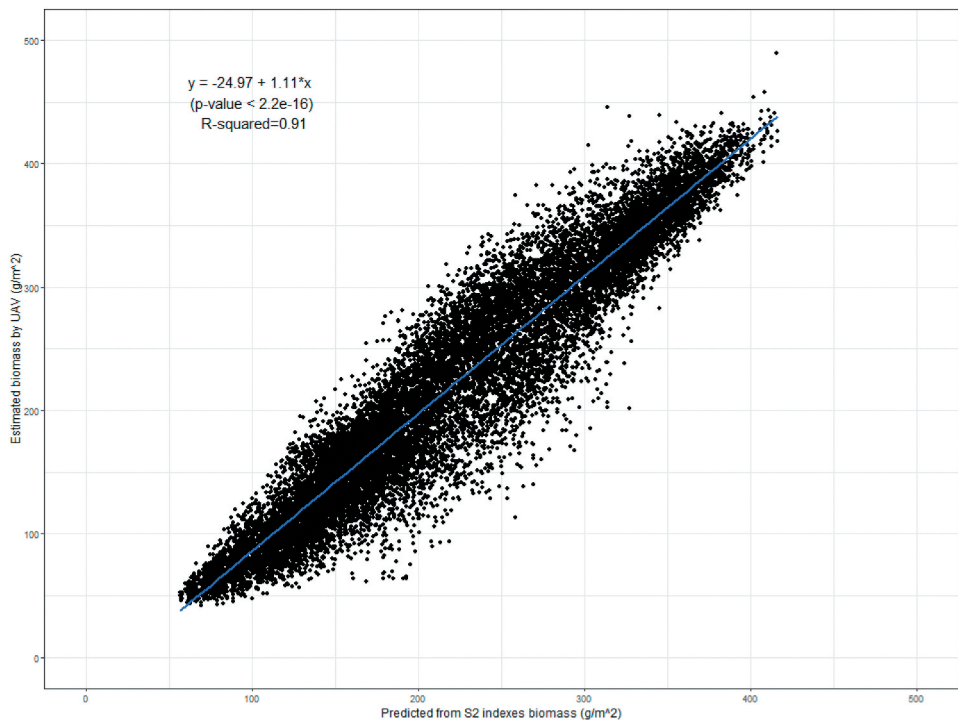


Figure 8. Relationship between dry mass estimated from UAV orthomosaics and the predictions from Sentinel-2 vegetation indices across the different sites (for 17,687 Sentinel-2 pixels).

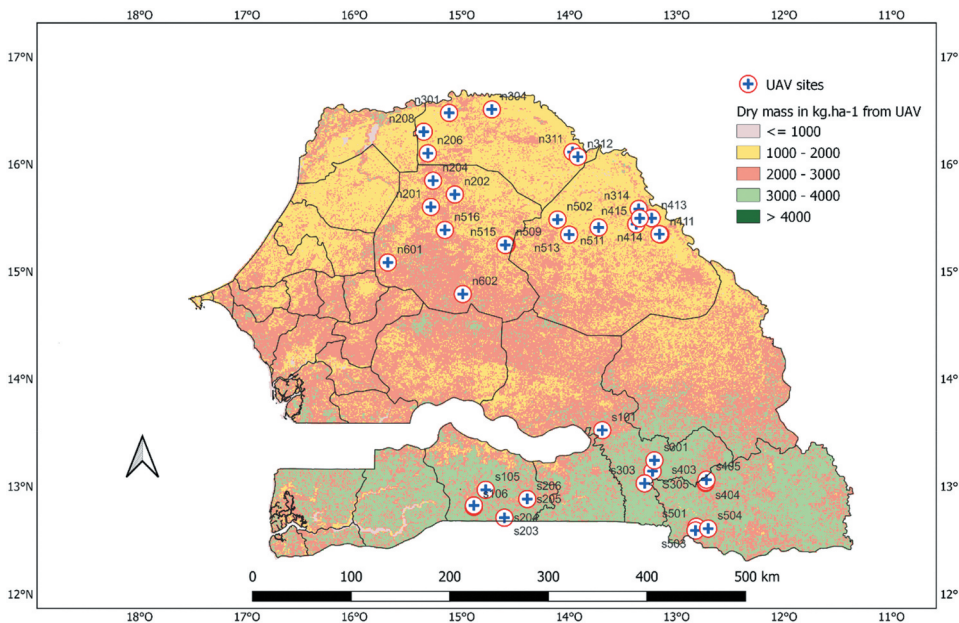


Figure 9. National-scale dry mass (kg.Ha.1) for Senegal obtained from the random forest model based on Sentinel-2 images trained by dry mass estimates from the UAV orthomosaics.

map). The highest dry mass reported in the CSE map was for the Kolda Region, with an average of 4,650 kg.ha-1.

The difference between UAV and CSE (Figure 10) showed that the UAV-based method produced higher values for the northern part of Senegal (the difference for the Saint Louis region was of 277 kg.ha-1) and for the Dakar Region (difference of 1,214.13 kg.ha-1). For all the other regions in Senegal, the UAV dry mass results obtained were lower than those of the CSE map (Table 2). The difference was relatively low for the Thies (-33.44 kg ha) and Diourbel (-142.32 kg.ha-1) regions, characterizing rainfall conditions approximately in the middle of the range between dry and wet conditions from North to South. For the five remaining regions, the differences were rather pronounced, as it was found to be around 1,000 kg ha for the Fatick, Kaolack and Ziguinchor regions. The two regions with the greatest difference were the Kolda and Tambacounda regions, with a difference of around 2,000 kg.ha-1.

In total, the UAV-based map featured 20 557 461t of dry mass less than the CSE map, with most of this difference arising from the Tambacounda and the Kolda regions in the southernmost part of the country.

4. Discussion

4.1. Methodological limitations

One limitation in this work was related to the quality of information derived from the data acquired from the UAV flights. When capturing the herbaceous dry mass, different aspects could have been improved to enhance quality (Taugourdeau et al. 2022). The first point is

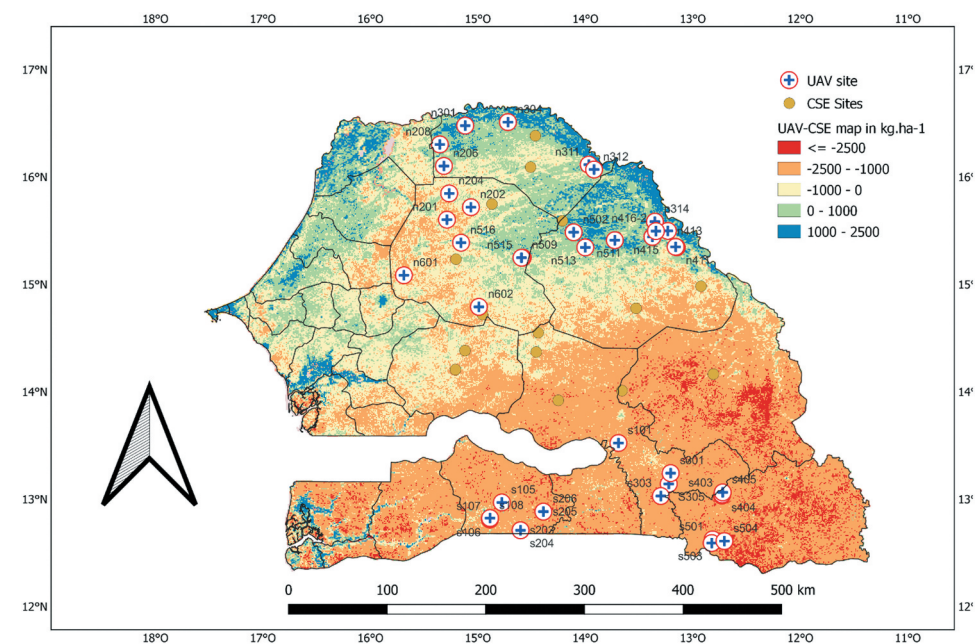


Figure 10. Difference between dry mass (kg.Ha-1) estimated by the UAV-based approach and that estimated by the CSE for 2020. Negative values correspond to the pixels with higher values in the CSE map than in the UAV-based map and vice versa.

Table 2. Average values in kg of dry mass and sum in tons of dry mass for each region of Senegal (Figure 1, 9 and 10) from the UAV-based and CSE map, respectively. The average and the sum of the differences between the two datasets are provided in the last column.

Region	UAV		CSE		UAV-CSE	
	Average in kg. ha-1	Sum in dry mass	Average in kg. ha-1	Sum in dry mass	Average in kg. ha-1	Sum in dry mass
Saint Louis	1 818	8 272 751	1 541	8 136 787	277	135 964
Louga	1 918	6 038 437	2 094	7 407 324	-175	-1 368 887
Diourbel	2 208	950 250	2 351	1 075 100	-142	-124 849
Thies	2 123	1 420 386	2 156	1 458 790	-33	-38 404
Dakar	2 003	122 635	789	72 875	1 214	49 761
Fatick	1 810	2 013 901	2 698	2 330 852	-888	-316 952
Kaolack	2 268	3 478 587	3 084	5 064 358	-816	-1 585 772
Tambacounda	2 618	15 775 762	4 429	28 234 873	-1 811	-12 459 111
Kolda	2 987	6 245 080	4 650	10 245 982	-1 663	-4 000 902
Ziguinchor	2 723	2 010 705	3 711	2 859 015	-988	-848 310
Total	2 244	46 328 495	2 924	66 885 956	-681	-20 557 461

related to the geographical position of the field measurements and the UAV imagery. In the dataset, we used a ground mark (white triangle on the ground), but it led to some inaccuracies in the geographical position of the measurements (small difference between the square and the triangle). Two solutions could potentially mitigate this problem: (a) One option is to conduct two UAV flights, with one conducted before the field measurements. The comparison between the two flights could then be used to define the position of the ground measurements more accurately. (b) Another possibility is to mark out a 1 m²

square that is visible in the UAV imagery. In that way, the whole square used to collect herbaceous dry mass will be visible for the UAV. The second point is related to the number of measurements used for model training. Here, we were limited to 86 measurements. An increase in the number of measurements could have improved the quality of the prediction, especially in this wide diversity of situations that characterizes the various landscape types across the North-South gradient in Senegal. Thirdly, we used a low-cost RGB UAV for this work. A UAV equipped with a sensor also measuring in the NIR spectral wavelengths, as used in many studies (Candiago et al. 2015; Geipel et al. 2021; Prošek and Šimová 2019), could have provided additional important spectral information for better characterization of herbaceous and woody vegetation. Few studies, however, have compared NIR and RGB UAV on grassland ecosystems (Schucknecht et al. 2022), but we expect that NIR UAV have a better prediction quality than the RGB UAV.

For the foliar dry mass of trees, the first limitation pertains to the method of estimating foliar mass on the ground. Indeed, the use of allometric equations involves some uncertainty. In the context of the current study, the problem arose especially in relation to the woody species in southern Senegal, where a generic allometric equation was used (Henry et al. 2011).

In terms of UAV mapping, one final challenge relates to the herbaceous cover below the tree crowns. It is well known that the herbaceous dry mass under tree crowns is greater than outside tree crowns (in the Sahel, mainly due to improved moisture and nutrient conditions (Akpo, Banoin, and Grouzis 2003)). In this work, we considered that for 1 m² grid cells that included both herbaceous and woody parts, the UAV indices, hence the dry mass of the herbaceous part, were representative of the area under the tree crowns. The potential error due to the herbaceous dry mass under the tree crowns is expected to be rather low for the savanna part of the country (northern part) with a general crown cover of 0–10% (Dendoncker and Vincke 2020). However, in the southern part of Senegal, some areas are characterized by dense forest with a very large percentage of tree cover and here this assumption and associated potential bias could be more critical.

During the rainy season, characterized by frequent cloud cover, high quality Sentinel-2 imagery is not necessarily available at every location on a national scale for every month. Use of time series images is especially useful in Sahelian countries where the vegetation cycle is different along the latitude (Diouf et al. 2017). One option could be to use other image sources, such as PlanetScope imagery characterized by a higher temporal and spatial resolution (Reiner et al. 2022). The original data is not freely available, which limits their operational use in developing countries. However, monthly composited PlanetScope data has been available since 2020 (made publicly available from the NICFI program (Norway's International Climate and Forests Initiative Satellite Data Program), which could be an interesting complementary data source to explore.

We found a good correlation between UAV dry mass and Sentinel 2 (Figure 8) even with the different limits we discuss. It means that the Sentinel 2 indices and UAV indices are related and so the part of dry mass explained by the UAV is strongly related to satellite images. One reason is that most of the prediction of dry mass are related to vegetation indices based on the reflectance and not a 3D structure.

4.2. Comparison with the CSE reference map

Our comparison with the dry mass reference for Senegal produced by CSE shows that our dataset produced higher dry mass estimates for the northern region. Data collection for the UAV map was carried out slightly earlier (end of September) than the CSE collection in 2020 (mid-October), which might have had an impact. At the end of the rainy season, dry mass quickly decreases with seed dispersion (Diawara et al. 2018). A small-time difference between two measurements during this period of the year could therefore greatly influence dry mass estimation, which might partly explain the difference we found. Furthermore, the difference could have been related to the type of satellite images used for the production of the two different map sources. We used a composite image from Sentinel-2, whereas CSE used more images during the rainy season from the NDVI 300 m V2 (Sentinel-3/OLCI) of the Copernicus Global Land Service (CGLS) platform.

In the southern region, the CSE map showed notably higher dry mass estimates than our combined UAV and Sentinel-2-based approach. One reason is likely to be the absence of CSE measurement sites in the southern part of Senegal. This part of the country is covered by a mosaic of very different types of vegetation; for example the Niokolo-Koba National Park has areas with dense forest close to rivers and water ponds, as well as densely forested savanna in a large part of the park (Madsen et al. 1996). In some other regions, the vegetation is a steppe type on ferrallitic soils, where vegetation is sparse. On the ferrallitic soil, the vegetation in the Kedougou region is to some extent similar, but with more topographic relief that has created a large variability in vegetation cover. Moreover, in the Kedougou region some areas are characterized by shifting cultivation (rotation of cultivation and fallow). In the Kolda and Ziguinchor regions, the land cover is dominated by forest, but often severely degraded by human activity (fire, cropping and grazing) and therefore the landscape is highly heterogenous in comparison to the landscapes further north (Kâ et al. 2020). Moderate resolution satellite images, such as the Sentinel-3 data used by CSE, are not always able to accurately resolve the characteristics of landscapes of such high spatial heterogeneity. The framework including UAV orthomosaics in combination with 10 m resolution Sentinel-2 data is well suited to this type of area in contrast to the use of a transect, as done by CSE. Indeed, the sampling protocol along a 1 km transect is not adapted to this type of landscape. The difference found in the central-eastern part of Senegal could also be due the difference in sampling, as UAV sites were not included in this region, whereas the CSE-based approach had several sites covering this region. Here, our approach would benefit from additional UAV measurements, to confirm the reason for the differences observed.

We cannot say which one of the two maps is the more accurate. An evaluation with a third dataset could be used to evaluate the quality of each method.

One notable difference between the two methods relates to the cost of the monitoring framework. We have made an approximate calculation of the cost of the two types of measurement designs (Table 3). UAV-based mapping relies on fewer measurements in the field requiring a smaller team for that purpose. Of course, UAV-based mapping requires the purchase of a UAV and the mapping software (here PIX4Dmapper), but even with this one-off expense, the cost remains lower than the costs associated with the regular mapping conducted by CSE. Such a UAV-based

Table 3. Budget estimation for the two different methods (in euro) for obtaining national-scale dry mass estimates.

	CSE			UAV-based mapping	
	Cost unit	Number	Cost	Number	Cost
Number of days' work	46	120	5,520	60	2,760
Km by car	2	7,500	15,000	3,000	6,000
Field equipment	150	5	750	2	300
UAV	500		0	1	500
Mapping software	1,550		0	1	1,550
		Total	21,270	Total	11,110

framework could therefore be a methodology that could be used in the different Sahelian countries by local authorities, but also by NGOs, to map dry mass on a regional scale.

Acknowledgements

This research was funded by the Carbon Sequestration and Green-house Gas Emissions in (Agro) Sylvopastoral Ecosystems in the Sahelian CILSS States (CaSSECS) project, supported by the European Union under the Development Smart Innovation through Research in Agriculture (DeSIRA) initiative. The opinions expressed in this article are not necessarily those of the European Union. This work was supported by the French National Research Agency under the Investments for the Future Programme #DigitAg, referred to as ANR-16-CONV- 0004. TT was additionally funded by Formas (Dnr. F 2021/718), and the Swedish National Space Agency (SNSA Dnr 95/16 and F2022/497).

Disclosure statement

No potential conflict of interest was reported by the author(s).

Funding

The work was supported by the Agence Nationale de la Recherche [ANR-16-CONV- 0004. TT]; Desira European Union [CaSSECS]; Svenska Forskningsrådet Formas [Dnr. F 2021/718]; Swedish National Space Agency [Dnr 95/16 and F2022/].

Data availability statement

The data used in the work are available in zenodo and described in Taugourdeau et al. (2023)

References

- Akpo, L., M. Banoin, and M. Grouzis. 2003. "Effet de l'arbre sur la production et la qualite fourrageres de la vegetation herbacee: bilan pastoral en milieu sahelien." *Revue de Médecine Vétérinaire* 154 (10): 619–628.
- Assouma, M., P. Lecomte, P. Hiernaux, A. Ickowicz, C. Corniaux, V. Decruyenaere, A. Diarra, and J. Vayssières. 2018. "How to Better Account for Livestock Diversity and Fodder Seasonality in Assessing the Fodder Intake of Livestock Grazing Semi-Arid Sub-Saharan Africa Rangelands." *Livestock Science* 216:16–23. <https://doi.org/10.1016/j.livsci.2018.07.002>.

- Ayantunde, A. A., P. Hiernaux, S. Fernández-Rivera, H. van Keulen, and H. M. J. Udo. 1999. "Selective Grazing by Cattle on Spatially and Seasonally Heterogeneous Rangeland in Sahel." *Journal of Arid Environments* 42 (4): 261–279. <https://doi.org/10.1006/jare.1999.0518>.
- Bassine, F. Z., A. Errami, and M. Khaldoun. 2019. "Vegetation recognition based on UAV image color index." In: *2019 IEEE International Conference on Environment and Electrical Engineering and 2019 IEEE Industrial and Commercial Power Systems Europe (IEEEIC/ICPS Europe)*, Genova, Italy (pp. 1–4). IEEE
- Bendig, J., K. Yu, H. Aasen, A. Bolten, S. Bennertz, J. Broscheit, M. L. Gnyp, and G. Bareth. 2015. "Combining UAV-Based Plant Height from Crop Surface Models, Visible, and Near Infrared Vegetation Indices for Biomass Monitoring in Barley." *International Journal of Applied Earth Observation and Geoinformation* 39:79–87. <https://doi.org/10.1016/j.jag.2015.02.012>.
- Bossoukpe, M., E. Faye, O. Ndiaye, S. Diatta, O. Diatta, A. Diouf, M. Dendoncker, M. H. Assouma, and S. Taugourdeau. 2021. "Low-Cost Drones Help Measure Tree Characteristics in the Sahelian Savanna." *Journal of Arid Environments* 187:104449. <https://doi.org/10.1016/j.jaridenv.2021.104449>.
- Bossoukpe, M., O. Ndiaye, O. Diatta, S. Diatta, A. Audebert, P. Couteron, L. Leroux, et al. 2021. "Unmanned Aerial Vehicle for the Assessment of Woody and Herbaceous Phytomass in Sahelian Savanna." *Revue d'élevage et de médecine vétérinaire des pays tropicaux* 74 (4): 199–205. <https://doi.org/10.19182/remvt.36802>.
- Brandt, M., C. J. Tucker, A. Kariryaa, K. Rasmussen, C. Abel, J. Small, J. Chave, L. V. Rasmussen, P. Hiernaux, and A. A. Diouf. 2020. "An Unexpectedly Large Count of Trees in the West African Sahara and Sahel." *Nature* 587 (7832): 78–82. <https://doi.org/10.1038/s41586-020-2824-5>.
- Breiman, L. 2001. "Random Forests." *Machine Learning* 45 (1): 5–32. <https://doi.org/10.1023/A:1010933404324>.
- Candiago, S., F. Remondino, M. De Giglio, M. Dubbini, and M. Gattelli. 2015. "Evaluating Multispectral Images and Vegetation Indices for Precision Farming Applications from UAV Images." *Remote Sensing* 7 (4): 4026–4047. <https://doi.org/10.3390/rs70404026>.
- Dendoncker, M., and C. Vincke. 2020. "Low Topographic Positions Enhance Woody Vegetation Stability in the Ferlo (Senegalese Sahel)." *Journal of Arid Environments* 175:104087. <https://doi.org/10.1016/j.jaridenv.2019.104087>.
- Diatta, O., D. Ngom, O. Ndiaye, S. Diatta, and S. Taugourdeau. 2023. "Structure and Phenology of Herbaceous Stratum in the Sahelian Rangelands of Senegal." *Grasses* 2 (2): 98–111. <https://doi.org/10.3390/grasses2020009>.
- Diawara, M. O., P. Hiernaux, E. Mougin, M. Grippa, C. Delon, and H. S. Diakité. 2018. "Effets de la pâture sur la dynamique de la végétation herbacée au Sahel (Gourma, Mali): une approche par modélisation." *Cahiers Agricultures* 27 (1): 15010. <https://doi.org/10.1051/cagri/2018002>.
- Diouf, A. A., M. Brandt, A. Verger, M. El Jarroudi, B. Djaby, R. Fensholt, J. A. Ndione, and B. Tychon. 2015. "Fodder Biomass Monitoring in Sahelian Rangelands Using Phenological Metrics from FAPAR Time Series." *Remote Sensing* 7 (7): 9122–9148. <https://doi.org/10.3390/rs70709122>.
- Diouf, A. A., P. Hiernaux, M. Brandt, G. Faye, B. Djaby, M. B. Diop, J. A. Ndione, and B. Tychon. 2016. "Do Agrometeorological Data Improve Optical Satellite-Based Estimations of the Herbaceous Yield in Sahelian Semi-Arid Ecosystems?" *Remote Sensing* 8 (8): 668. <https://doi.org/10.3390/rs8080668>.
- Diouf, A. A., M. A. Sarr, T. Ba, S. Taugourdeau, A. M. Dieye, I. Sy, and A. T. Diop. 2017. "Évaluation intra-saisonnière de la production fourragère des parcours naturels du Sénégal." In *Pastoralisme dans le courant des changements globaux: Défis, enjeux, perspectives*, 2. Dakar, Sénégal: PPZS.
- Ezanno, P., A. Ickowicz, and F. Bocquier. 2003. "Factors Affecting the Body Condition Score of N'dama Cows Under Extensive Range Management in Southern Senegal." *Animal Research* 52 (1): 37–48. <https://doi.org/10.1051/animres:2003002>.
- Fassinou, C., A. A. J. N'Goran, O. Diatta, D. Diatta, O. Ndiaye, and S. Taugourdeau. 2022. "Impact of Tree on the Growth of the Herbaceous Layer of Sahelian Savannah. A UAV Based Approach." In *29th EGF general meeting: Grassland at the heart of circular and sustainable food systems*, Caen, EGF.
- Fensholt, R., and K. Rasmussen. 2011. "Analysis of Trends in the Sahelian 'Rain-Use Efficiency' using GIMMS NDVI, RFE and GPCP Rainfall Data." *Remote Sensing of Environment* 115 (2): 438–451. <https://doi.org/10.1016/j.rse.2010.09.014>.

- Fensholt, R., K. Rasmussen, T. T. Nielsen, and C. Mbow. 2009. "Evaluation of Earth Observation Based Long Term Vegetation Trends—Intercomparing NDVI Time Series Trend Analysis Consistency of Sahel from AVHRR GIMMS, Terra MODIS and SPOT VGT Data." *Remote Sensing of Environment* 113 (9): 1886–1898. <https://doi.org/10.1016/j.rse.2009.04.004>.
- Garba, I., B. Djaby, I. Salifou, I. Samba, A. Toure, Y. Yapo, A. Agoumo, S. Soumana, A. Oumarou, and B. Tychon. 2017. "MAPPING OF ZONES AT RISK (ZAR) IN WEST AFRICABY USING NGI, VCI AND SNDVI FROM THE E-STATION." *International Journal of Advanced Research* 5 (4): 1377–1386. <https://doi.org/10.21474/IJAR01/3953>.
- Gaston, A., and G. Lamarque. 1994. "Les pâturages sahéliens de l'Afrique de l'Ouest. Extraits des atlas "Elevage et potentialités pastorales sahéliennes"." In *7 Annexes cartographiques*, edited by N. Tchad, B. Faso, and S. M. Mali, 221. Maisons-Alfort, France: CIRAD-EMVT.
- Geipel, J., A. K. Bakken, M. Jørgensen, and A. Korsæth. 2021. "Forage Yield and Quality Estimation by Means of UAV and Hyperspectral Imaging." *Precision Agriculture* 22 (5): 1437–1463. <https://doi.org/10.1007/s11119-021-09790-2>.
- Grenzdörffer, G., A. Engel, and B. Teichert. 2008. "The Photogrammetric Potential of Low-Cost UAVs in Forestry and Agriculture." *The International Archives of the Photogrammetry, Remote Sensing and Spatial Information Sciences* 31 (B3): 1207–1214.
- Hanan, N. P., E. Milne, E. Aynekulu, Q. Yu, and J. Anchang. 2021. "A Role for Drylands in a Carbon Neutral World?" *Frontiers in Environmental Science* 9:539. <https://doi.org/10.3389/fenvs.2021.786087>.
- Henry, M., N. Picard, C. Trotta, R. Manlay, R. Valentini, M. Bernoux, and L. Saint André. 2011. "Estimating Tree Biomass of Sub-Saharan African Forests: A Review of Available Allometric Equations." *Silva Fennica* 45 (3B): 477–569. <https://doi.org/10.14214/sf.38>.
- Hiernaux, P., M. Wele, I. Garba, I. Touré, B. Diaby, A. Ickowicz, A. Seck-Diallo, F. Camra, and I. Salifou. 2016. *Suivi-évaluation des parcours*, 11. s.l., Autre: s.n.
- Janowiak, J. E. 1988. "An Investigation of Interannual Rainfall Variability in Africa." *Journal of Climate* 1 (3): 240–255. [https://doi.org/10.1175/1520-0442\(1988\)001<0240:AIOIRV>2.0.CO;2](https://doi.org/10.1175/1520-0442(1988)001<0240:AIOIRV>2.0.CO;2).
- Kâ, S. L., M. O. Ly, M. Diouf, M. Diandy, M. Guéye, M. S. Mbaye, and K. Noba. 2020. "Diversité herbacée dans les parcours du noyau de sélection du Centre de recherches zootechniques de Kolda en zone soudanienne du Sénégal." *Revue d'élevage et de médecine vétérinaire des pays tropicaux* 73 (3): 199–205. <https://doi.org/10.19182/remvt.31891>.
- Kaneko, K., and S. Nohara. 2014. "Review of Effective Vegetation Mapping Using the UAV (Unmanned Aerial Vehicle) Method." *Journal of Geographic Information System* 6 (6): 733. <https://doi.org/10.4236/jgis.2014.66060>.
- Le Houerou, H. N. 1980. "The Rangelands of the Sahel." *Journal of Range Management* 33 (1): 41–46. <https://doi.org/10.2307/3898226>.
- L'Hôte, Y., G. Mahé, B. Somé, and J. P. Triboulet. 2002. "Analysis of a Sahelian Annual Rainfall Index from 1896 to 2000; the Drought Continues." *Hydrological Sciences Journal* 47 (4): 563–572. <https://doi.org/10.1080/02626660209492960>.
- Lo, A., A. A. Diouf, I. Diédhiou, C. D. E. Bassène, L. Leroux, T. Tagesson, R. Fensholt, P. Hiernaux, A. Mottet, and S. Taugourdeau. 2022. "Dry Season Forage Assessment Across Senegalese Rangelands Using Earth Observation Data." *Frontiers in Environmental Science* 10. <https://doi.org/10.3389/fenvs.2022.931299>.
- Lussem, U., A. Bolten, M. Gnyp, J. Jasper, and G. Bareth. 2018. "Evaluation of RGB-Based Vegetation Indices from UAV Imagery to Estimate Forage Yield in Grassland." *The International Archives of the Photogrammetry, Remote Sensing and Spatial Information Sciences* XLII-3:1215–1219. <https://doi.org/10.5194/isprs-archives-XLII-3-1215-2018>.
- Madsen, J., D. Dione, A. Traoré, and B. Sambou. 1996. "Flora and Vegetation of Niokolo-Koba National Park, Senegal." In *The Biodiversity of African Plants*, edited by S. van Wageningen, 214–219. Springer.
- Mayr, M. J., S. Malß, E. Ofner, and C. Samimi. 2018. "Disturbance Feedbacks on the Height of Woody Vegetation in a Savannah: A Multi-Plot Assessment Using an Unmanned Aerial Vehicle (UAV)." *International Journal of Remote Sensing* 39 (14): 4761–4785. <https://doi.org/10.1080/01431161.2017.1362132>.

- Prošek, J., and P. Šimová. 2019. "UAV for Mapping Shrubland Vegetation: Does Fusion of Spectral and Vertical Information Derived from a Single Sensor Increase the Classification Accuracy?" *International Journal of Applied Earth Observation and Geoinformation* 75:151–162. <https://doi.org/10.1016/j.jag.2018.10.009>.
- Reiner, F., M. Brandt, X. Tong, D. Skole, A. Kariryaa, P. Ciais, A. Davies, P. Hiernaux, J. Chave, and M. Mugabowindekwe. 2022. *More Than One Quarter of Africa's Tree Cover Found Outside Areas Previously Classified as Forest* 14 (1): 2258.
- Rouse, J. W., R. H. Haas, J. A. Schell, and D. W. Deering. 1973. "Monitoring Vegetation Systems in the Great Plains with ERTS." In *Third ERTS Symposium*, SP-351. 309. Washington, D. C: NASA.
- Schucknecht, A., B. Seo, A. Krämer, S. Asam, C. Atzberger, and R. Kiese. 2022. "Estimating Dry Biomass and Plant Nitrogen Concentration in Pre-Alpine Grasslands with Low-Cost UAS-Borne Multispectral Data—A Comparison of Sensors, Algorithms, and Predictor Sets." *Biogeosciences* 19 (10): 2699–2727. <https://doi.org/10.5194/bg-19-2699-2022>.
- Tappan, G. G., M. Sall, E. C. Wood, and M. Cushing. 2004. "Ecoregions and Land Cover Trends in Senegal." *Journal of Arid Environments* 59 (3): 427–462. <https://doi.org/10.1016/j.jaridenv.2004.03.018>.
- Taugourdeau, S., F. Cofélas, M. Bossoukpe, O. Diatta, O. Ndiaye, A. Diehdiou, A. N'Goran, A. Audebert, and E. Faye. 2023. "Unmanned Aerial Vehicle Outputs and Associated Field Measurements of the Herbaceous and Tree Layers of the Senegalese Savannah." *African Journal of Ecology* 61 (3): 730–735. <https://doi.org/10.1111/aje.13123>.
- Taugourdeau, S., A. Diehdiou, C. Fassinou, M. Bossoukpe, O. Diatta, A. N'goran, A. Audebert, O. Ndiaye, A. A. Diouf, and T. Tagesson. 2022. "Estimating Herbaceous Aboveground Biomass in Sahelian Rangelands Using Structure from Motion Data Collected on the Ground and by UAV." *Ecology and Evolution* 12 (5): e8867. <https://doi.org/10.1002/ece3.8867>.
- Taugourdeau, S., G. Le Maire, J. Avelino, J. R. Jones, L. G. Ramirez, M. Jara Quesada, F. Charbonnier, et al. 2014. "Leaf Area Index as an Indicator of Ecosystem Services and Management Practices: An Application for Coffee Agroforestry." *Agriculture, Ecosystems and Environment* 192:19–37. <https://doi.org/10.1016/j.agee.2014.03.042>.
- Touré, I., and A. Ickowicz. 2014. "SIPSA : un système d'information et d'alerte précoce pour caractériser et suivre les dynamiques pastorales au Sahel." In *Élevages et territoires : Concepts, méthodes, outils*, edited by M. Etienne, 207–216. Paris, France: INRA.
- Wessels, K. J., M. Colgan, B. F. N. Erasmus, G. Asner, W. Twine, R. Mathieu, J. Van Aardt, J. Fisher, and I. P. Smit. 2013. "Unsustainable Fuelwood Extraction from South African Savannas." *Environmental Research Letters* 8 (1): 014007. <https://doi.org/10.1088/1748-9326/8/1/014007>.
- Wijesingha, J., T. Astor, D. Schulze-Brüninghoff, M. Wengert, and M. Wachendorf. 2020. "Predicting Forage Quality of Grasslands Using UAV-Borne Imaging Spectroscopy." *Remote Sensing* 12 (1): 126. <https://doi.org/10.3390/rs12010126>.